

Available online at www.sciencedirect.com**ScienceDirect**

Energy Procedia 70 (2015) 445 – 453

Energy

Procedia

International Conference on Solar Heating and Cooling for Buildings and Industry, SHC 2014

Integration of sorption modules in Sydney type vacuum tube collector with air as heat transfer fluid

Olof Hallstrom^a, Gerrit Földner^b^a Mälardalen University, Mälardalens högskola, Box 883, 721 23 Västerås, Sweden^b Fraunhofer-Institut für Solare Energiesysteme ISE, Heidenhofstraße 2, 79110 Freiburg, Germany

Abstract

Reduced thermal losses and simplified system integration have previously been identified as main opportunities to improve the concept of collector integrated sorption modules for solar heating and cooling. A concept for a façade integrated sorption collector using Sydney type vacuum tube technology and air based heat transfer has been developed and tested in the laboratory. The results from the tests have been used to validate an existing TRNSYS model that has been modified for use with air as heat transfer fluid. The work has been conducted within the FP7 EU iNSPiRe project with the aim to develop a plug & play solar cooling and heating solution.

© 2015 The Authors. Published by Elsevier Ltd. This is an open access article under the CC BY-NC-ND license (<http://creativecommons.org/licenses/by-nc-nd/4.0/>).

Peer-review by the scientific conference committee of SHC 2014 under responsibility of PSE AG

Keywords: solar cooling, absorption, integrated sorption collector, sorption heat pump, air collector

1. Introduction

Solar thermal cooling has difficulty in emerging as an economically viable solution for small-scale systems mainly due to high investment costs and system complexity [1]. A collector integrated sorption system was proposed as one solution to this issue in 2013 [2]. The paper concluded that the collector losses were the main efficiency driver and hence the area of most interest for further research. The collector integrated concept has thus been developed further with focus on reducing collector losses and simplifying system integration. The main idea has been to use air as heat transfer medium with the goal to integrate the collector into the façade of buildings and deliver heating and cooling directly to the conditioned space or to the outdoor environment (heat rejection).

Nomenclature

$\eta_0, \eta_{a_0}, a_1, a_2$	Collector efficiency parameters
η, η_a	Total efficiency of collector (-)
η_{cool}, η_{cool}	Thermal cooling efficiency of the collector (cooling energy, kWh/ total insolation, kWh)
η_{heat}, η_{heat}	Thermal heating efficiency of the collector (heating energy, kWh/ total insolation, kWh)
R	Heat transfer resistance (inverse of UA) (K/W)
solar	Heat input (kJ/hr)
N_{tube}	Number of sorption modules in a collector (-)
T_{re}	Internal temperature of reactor (salt solution) (°C)
T_{ce}	Internal temperature of condenser/evaporator (refrigerant) (°C)
$T_{re,abs}$	Temperature of reactor heat exchanger node (absorber) (°C)
$T_{ce,abs}$	Temperature of condenser/evaporator (C/E) heat exchanger node (°C)
$T_{rx,i}, T_{rx,o}$	Inlet/Outlet temperature to reactor heat exchanger, after manifold losses (°C)
$T_{cx,i}, T_{cx,o}$	Inlet/Outlet temperature to condenser/evaporator (C/E) heat exchanger, after manifold losses (°C)
$T_{su,rx,i}, T_{su,rx,o}$	Inlet/Outlet temperature to reactor heat exchanger, before manifold losses (°C)
$T_{su,cx,i}, T_{su,cx,o}$	Inlet/Outlet temperature to C/E heat exchanger, before manifold losses (°C)
$C_{re,abs}$	Thermal mass of reactor absorber (kJ/K)
$C_{re,ins}$	Thermal mass of reactor absorber insulation (collector casing) (kJ/K)
UA_{rx}	Heat transfer coefficient between fluid loop and reactor absorber (W/K)
UA_{cx}	Heat transfer coefficient between fluid loop and condenser/evaporator absorber (W/K)
$UA_{re,abs}$	Heat transfer coefficient between reactor absorber and reactor (W/K)
$UA_{ce,abs}$	Heat transfer coefficient between condenser/evaporator absorber and condenser/evaporator (W/K)
$UA_{re,abs,ins}$	Heat transfer coefficient between reactor absorber and reactor insulation (collector casing) (W/K)
$UA_{ins,amb}$	Heat transfer coefficient between reactor insulation and ambient (outer Sydney tube) (W/K)
$UA_{rx,amb}$	Heat transfer coefficient between reactor manifold and ambient (W/K)
$UA_{cx,amb}$	Heat transfer coefficient between condenser/evaporator manifold and ambient (W/K)
UA_{int}	Internal heat transfer coefficient between reactor and condenser/evaporator (W/K)

2. Method

Sorption tubes based on LiCl and water have been integrated into a Sydney type vacuum collector. CFD simulations in combination with small scale lab tests have been used to develop aluminium heat exchangers that can efficiently heat and cool both parts of the sorption tube (reactor and condenser/evaporator). A full scale collector consisting of 4 sorption tubes has been manufactured and tested in a solar simulator. An existing mathematical model for TRNSYS environment has been adapted for air heat transfer and validated based on the measurements. The model has then been used to find key performance indicators.

The sorption modules are identical to the ones used in [2]. A salt solution of LiCl and water is used to create a temperature difference between the reactor and the condenser/evaporator part of the module. Vapour can flow from the salt solution in the reactor to the condenser/evaporator if heat is supplied to the reactor and rejected from the condenser/evaporator in such a way that the pressure is maintained higher on the salt side of the module. Vapour will go the other way as soon as heat is no longer supplied to the reactor and the salt solution temperature is sufficiently low.

The idea behind the collector integration has been to minimize the number of components and to use standard components as far as possible. The main component of the collector is the Sydney tube which is not only used to capture solar irradiation and minimizing thermal losses, but is also a structural component for directing the air flow. Since the Sydney tube is only open in one end, air must enter on one side of the circular gap, make a bend at the bottom of the tube, and exit through the other side of the gap. The configuration of the inlet and outlet is illustrated in Fig. 2. The heat exchangers must be able to reject/supply heat efficiently without producing too high pressure drops. In addition the reactor heat exchanger must also during desorption be able to conduct heat from the inner pipe of the Sydney tube to the sorption tube across the air gap. The target for the heat exchangers is to have no more than 30Pa of pressure drop at nominal flow and to perform similar to a water based collector in regards to cooling and heating powers. Higher pressure drops than 30Pa would lead to too much parasitic electric consumption. The design of the heat exchangers has been made in an iterative process. In a first step CFD modelling was performed on a preliminary heat exchanger design using standard Sydney tube dimensions. The model was then validated against measurements for a first single module prototype. Based on those results a larger diameter Sydney tube was chosen due to high initial pressure drops. With the larger air gap a second heat exchanger design was simulated with good results leading to the manufacturing of the full scale prototype using the adjusted heat exchanger design. The C/E heat exchanger was not modelled with CFD. Due to the short length of the condenser/evaporator (C/E) a standard brazed micro channel lamella from Parker with 3mm height and staggard fins was used. The air only passes the lamella once and all lamellas are connected in parallel.

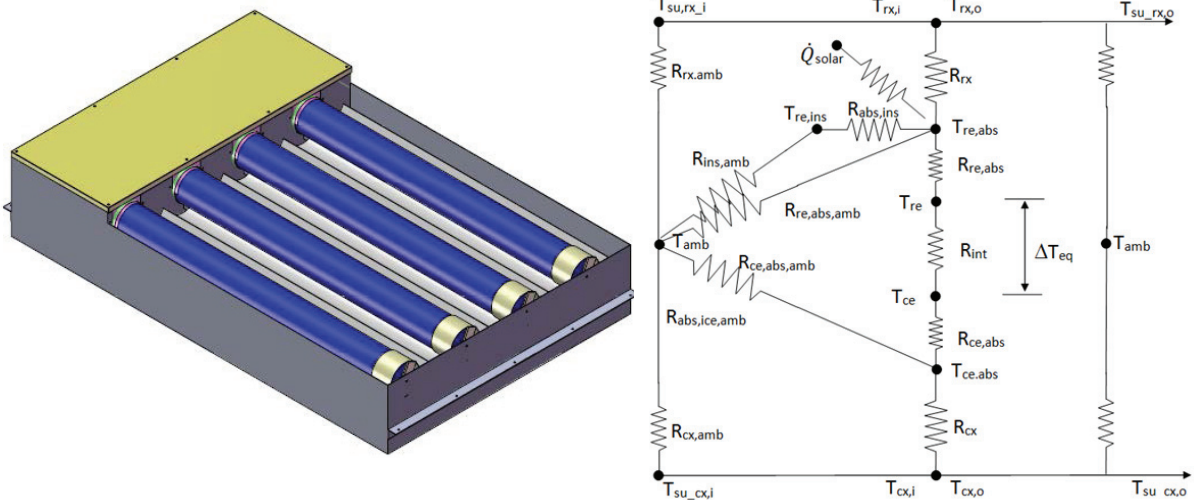


Fig. 1: Layout of the prototype collector (left). The lowest reflector has been truncated due to shadowing effects in the façade. Resistance network for the TRNSYS model (right). The model includes thermal mass for five independent thermal nodes.

The center-center (C-C) distance between individual sorption tubes determines the energy storage density of the collector and must be adjusted in accordance to the expected heat capture of the collector. Important parameters to consider for a correct dimensioning are climate, collector performance and collector orientation. Since the collector is meant to be used on a façade that receives considerably less insolation compared to a roof based collector the C-C distance must be larger. The validated model from [2] has been used to estimate a suitable C-C distance of 220mm (120mm for roof based flat plate) assuming standard vacuum tube performance parameters and a vertically installed, south oriented collector in Verona, Italy.

Once the Sydney tube dimensions and the sorption tube C-C distance were determined, a reflector could be designed. The design was made assuming horizontal Sydney tubes installed on a vertical southern façade in Verona with an 8mm aesthetic glazing covering the collector. Different types of reflectors were compared by ray tracing simulations and a symmetrical involute reflector was determined to have the best overall performance. The collector design is depicted in Fig. 1.

The details of the collector integration into a façade as well as a complete system solution with fans, ducting and dampers will be done in the continuation of the EU FP7 Inspire project (www.fp7inspire.eu). Only a brief introduction to the system approach will hence be described here. The main operation modes are identical to roof based sorption collectors; desorption is done during incident irradiation with flow through the C/E heat exchanger, cool down is done after desorption is finished by running fluid through the reactor heat exchanger, and cool down is followed by absorption with flow through both the reactor and C/E heat exchangers [2], [4], [5]. The season will decide where the heating and cooling is delivered. In cooling mode the condensation heat from the C/E heat exchanger during desorption will be rejected to the outside (step 4 below). During cool down and absorption the heat produced in the reactor is rejected to the outside (step 2 below) while the cooling produced in the C/E is channeled to the indoor environment (step 3 below). In addition the collector can of course be used as a conventional solar collector, harvesting the heat from the reactor during incident irradiation and delivering it to the indoor environment (step 1 below). In total there are four possible operation conditions for the air flow:

1. Indoor air passes through the reactor heat exchangers and is returned to the building.
2. Outdoor air passes through the reactor heat exchangers and is rejected to ambient.
3. Indoor air passes through the C/E heat exchangers and is returned to the building.
4. Outdoor air passes through the C/E heat exchangers and is rejected to ambient.

All of these possibilities are needed for a fully functional system that can give:

1. Heating from the reactor to the building (conventional solar collector).
2. Heat rejection from the reactor; absorption (cooling mode).
3. Cooling from the C/E to the building; absorption (cooling mode).
4. Heat rejection from the C/E; desorption (cooling mode).

In addition to these there is also the possibility of having a cross flow so that outdoor air is conditioned (cooled through the C/E) and sent to the indoor environment while moving the same amount of indoor air through the reactor to the outdoor environment. This last operation mode could potentially provide efficient free cooling and air renovation to the building in case the outdoor temperature is below the indoor.

The testing of the prototype collector has been performed in the solar simulator at Fraunhofer Institute for Solar Energy Systems (ISE). The collector was set up perpendicular to the solar lamps and connected to air inlet and outlet on both reactor and C/E side. The testing was conducted in a similar manner to previous sorption collector test. The test method is described in [2] and [3]. The main difference to previous tests is the humidity ratio of the incoming air that has to be taken into account. During absorption the outlet C/E temperature is sometimes below the dew point and condensation hence occurs within the collector. Since the model does not have a humidity input, the change in humidity ratio between inlet and outlet must be recalculated into latent cooling power, and then converted into additional heat capacity for the air flow. Four different types of steady state measurements have been used to calculate the optical efficiency as well as all thermal loss coefficient of the model, i.e. reactor tube losses, reactor manifold losses, C/E manifold losses, and internal losses. The loss equations in the model are shown in Eq. 1-5. Among the steady state measurements were conventional stagnation tests at 600 and 800 Wm⁻² respectively. For fitting the dynamic behaviour of the sorption modules an additional 10 dynamic cycle tests of desorption/absorption with varying solar intensity (600, 800 W/m²), and flows (20, 40, 60, 80m³/hrs) were performed. The UA-values in Eq. 1-5 are the inverses of the thermal resistances illustrated in Fig. 1.

Reactor absorber losses ($R_{abs,ins}$):

$$q_{re,abs,ins} = (UA_{re,abs,ins} + UA_{re,abs,ins2} * (T_{re,abs} - T_{re,ins})) * (T_{re,abs} - T_{re,ins}) \quad \text{Eq. 1}$$

Reactor insulation losses ($R_{ins,amb}$):

$$q_{ins,amb} = UA_{ins,amb} * (T_{re,ins} - T_{amb}) \quad \text{Eq. 2}$$

Reactor manifold losses ($R_{rx,amb}$):

$$q_{rx,amb} = UA_{rx,amb} * (T_{su,rx,o} + T_{su,rx,i} - 2 * T_{amb}) \quad \text{Eq. 3}$$

Reactor-C/E internal losses (R_{int}):

$$q_{loss,int} = UA_{int} * (T_{re,abs} - T_{ce,abs}) \quad \text{Eq. 4}$$

C/E manifold losses ($R_{cx,amb}$):

$$q_{cx,amb} = UA_{cx,amb} * (T_{su,cx,o} + T_{su,cx,i} - 2 * T_{amb}) \tag{Eq. 5}$$

The heat transfer resistances R_{rx} , R_{cx} , $R_{re,abs}$, and $R_{ce,abs}$ in Fig. 1 are determined from the dynamic measurements in combination with previous tests and CFD modelling. From the static measurements most of the heat transfer coefficients are determined. Other parameters for the model such as masses and thermal masses can be measured during the manufacturing of the sorption tubes (amount salt solution, water etc.) or calculated based on material, thickness and geometry. What remain to be determined are parameters governing the dynamic behaviour such as the mass transport resistance between reactor and C/E. These parameters are determined empirically by comparing the model to the dynamic measurements.

A sensitivity study was performed to find key performance indicators (KPI) as well as estimating error ranges for the model. An east oriented vertical façade was selected for the base case simulation. The entire month of July was simulated for two locations with different climates. By selecting a range around the fitted value for every parameter and simulating using the minimum and maximum value of this range while keeping the other parameters constant, the effect of each individual parameter can be seen. For simplicity the minimum and maximum values for most parameters were selected by either multiplying or dividing with a factor of 3. See Fig. 6 for details on the parameters varied in the sensitivity study.

3. Results

The results from the CFD modelling and the measurements on the first reactor heat exchanger design is presented in Fig. 2. Measured pressure drop was a factor 2 too high, but gave useful information to validate the CFD model.

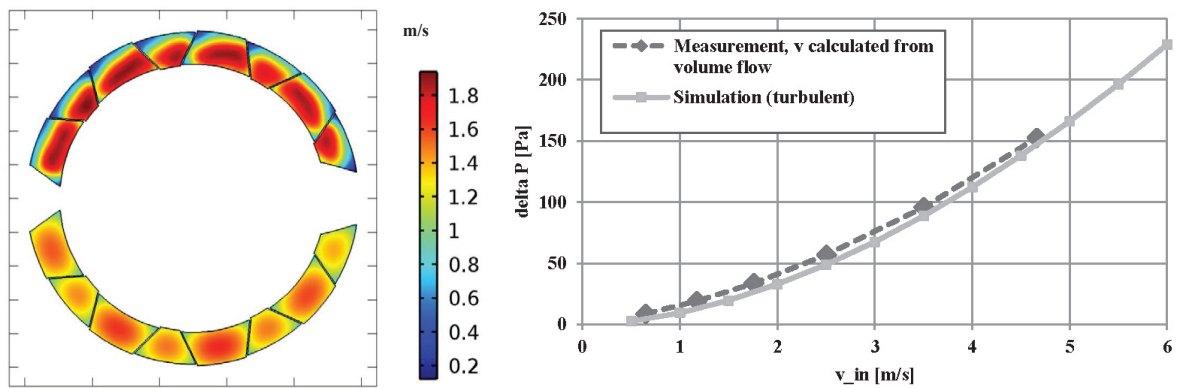


Fig. 2: Simulated velocity distribution at tube inlet and outlet for the first heat exchanger design at 0.5m/s manifold inlet velocity (left). Simulated and measured pressure drop for the first prototype (right). Nominal flow would mean a velocity of 2.4 m/s for the first design.

Based on the results in Fig. 2 a larger diameter Sydney tube was used for the full scale prototype. Measured pressure drop on the collector is shown in Fig. 3.

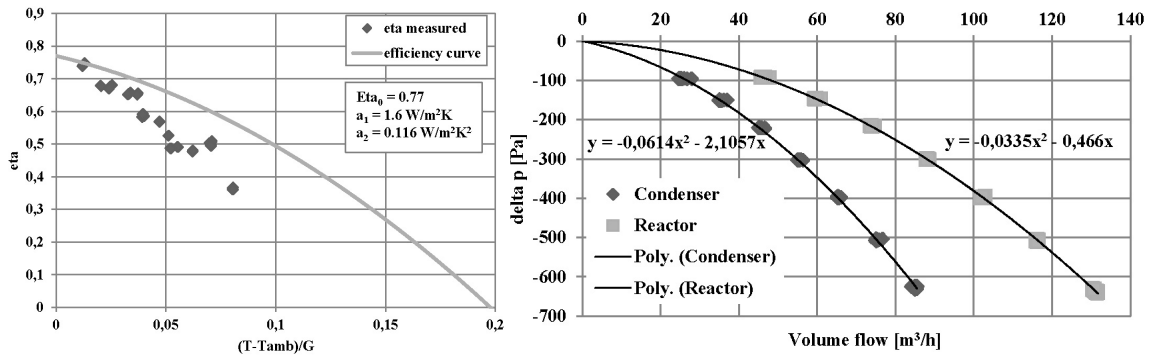


Fig. 3: Efficiency measurements with reactor flow and efficiency curve based on η_0 and the stagnation measurements (left). Measured pressure drop on reactor and C/E for the full scale collector (right). Nominal flow is $25\text{m}^3/\text{h}$ giving a velocity of 1.4 m/s at the entrance of each reactor tube inlet and 2.4 m/s at the entrance of each C/E tube inlet.

Simulated incidence angle modifiers (IAM) for the full scale collector are illustrated in Fig. 4.

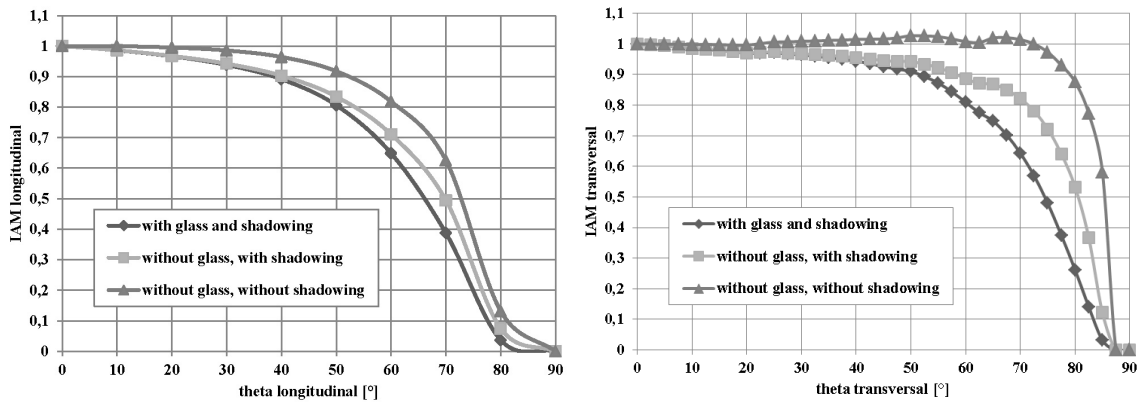


Fig. 4: Simulated transversal and longitudinal IAM-values of the Sydney tubes with reflector. The optical losses from the front glazing and shadow effects from the façade are quite significant.

The results from the efficiency- and stagnation measurements are illustrated in Fig. 3. η_0 is given from the efficiency measurements in Fig. 3 and in combination with the stagnation measurements, a_1 and a_2 can be determined. The difference between the line and the points in Fig. 3 is due to reactor manifold losses.

The results from the dynamic test cycles are shown in Table 1. Cooling and heating efficiencies (η_{cool} , η_{heat}) are similar to the results presented in [3].

Table 1: Energy, and heating and cooling efficiency for the 10 dynamic test measurements and the corresponding simulation outputs. The suffixes refer to solar insolation, condensation, cooling, and absorption respectively. The model over-predicts the condensation energy and under-predicts the cooling energy with on average 5%.

Measured cycles		1	2	3	4	5	6	7	8	9	10
Qsolar	Measured/Simulated	3.8	4.4	4.0	4.1	3.9	3.9	6.7	4.0	3.6	4.3
	Measured	0.89	0.87	0.86	0.88	0.86	0.87	0.94	0.87	0.89	0.95
Qcond	Simulated	0.94	0.85	0.94	0.94	0.93	0.94	0.97	0.93	0.92	0.95
	Measured	0.84	0.76	0.75	0.71	0.74	0.77	0.81	0.86	0.84	0.73
Qcool	Simulated	0.69	0.68	0.73	0.73	0.73	0.77	0.77	0.78	0.76	0.74
	Measured	1.4	1.3	1.1	1.2	1.1	1.1	2.6	1.2	1.1	1.0
Qabs	Simulated	1.1	1.2	1.1	1.2	1.2	1.0	2.7	1.2	1.0	1.0
	Measured	22	17	18	17	19	20	12	22	24	17
Eta _{cool}	Simulated	18	15	18	18	18	20	11	20	22	17
	Measured	59	49	48	51	49	50	53	53	56	46
Eta _{heat}	Simulated	55	47	50	51	53	50	54	54	55	45

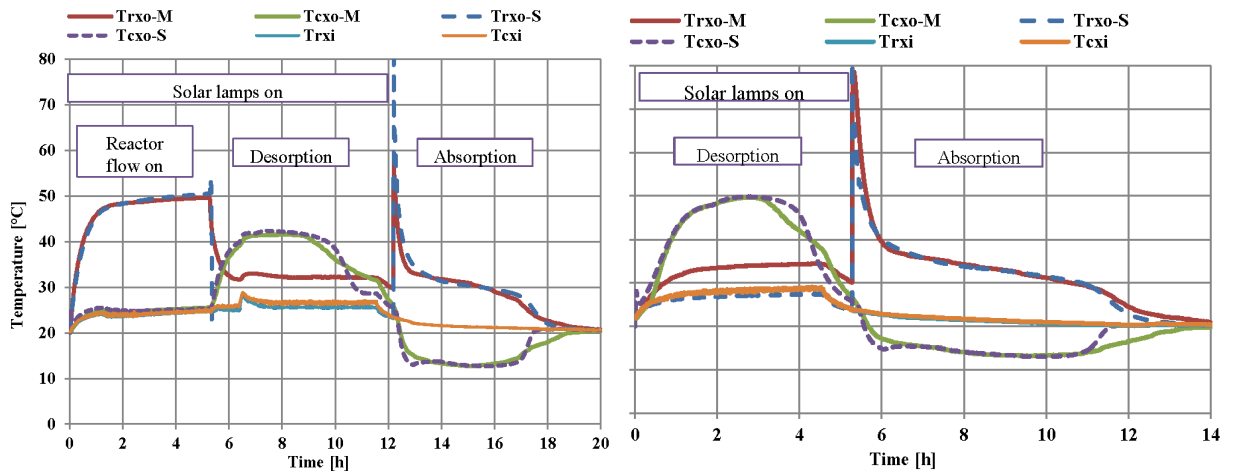


Fig. 5: Fitting of model to dynamic test measurements. Inlet flows and temperatures from the measurement are fed into the model and simulated (S) outlet temperatures are compared to measured (M).

Two examples from the parameter identification can be seen in Fig. 5. The model can fit the measured data well. The reactor heat exchange coefficient (UA_{rx}) increases with higher flow, while the UA_{cx} is fairly constant regardless of the flow. The worst fit is achieved towards the end of both desorption and absorption. The poor fit towards the end of desorption is believed to be due to differences in optical efficiency between the four individual sorption tubes in the collector, and very difficult to fit to a one-node model. The slow decrease in cooling power at the end of absorption could be condensed water on the heat exchanger surface re-evaporating and chilling the air.

The results from the sensitivity study are shown in Fig. 6.

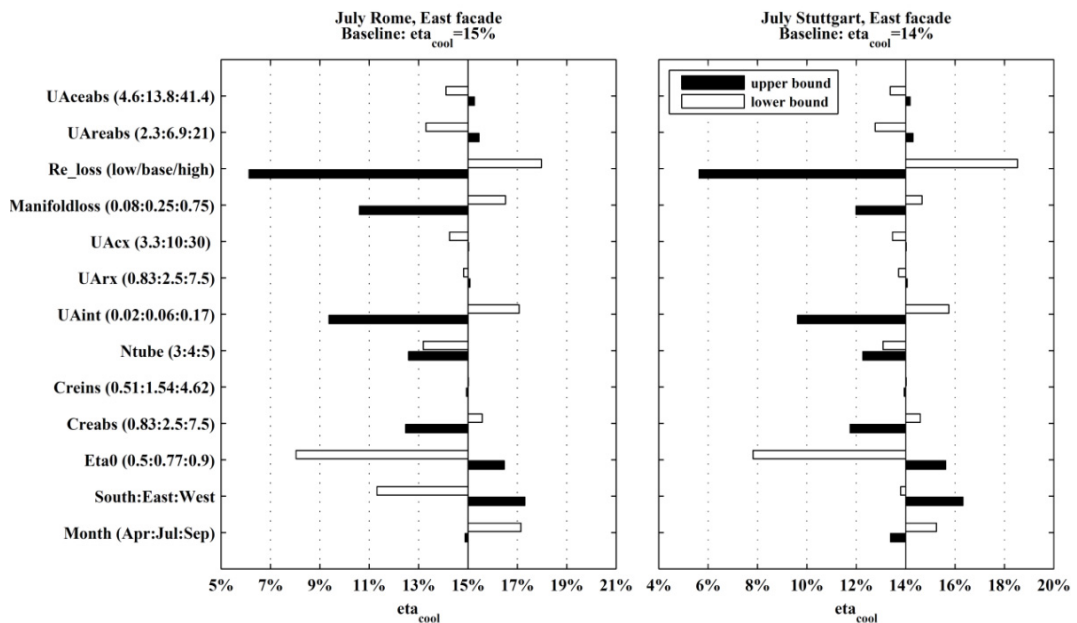


Fig. 6: Sensitivity study for the month of July in Rome and Stuttgart. The horizontal bars indicate the change in thermal efficiency in percentage of the base case (middle value). Re_loss refers to all parameters coupled to the reactor tube losses. Manifoldloss refers to the two parameters $UA_{rx,amb}$ and $UA_{cx,amb}$.

4. Discussion

The presented results clearly show that the concept of an air cooled/heated sorption collector for façade integration is promising. The challenge lies in two main aspects. Firstly the system concept must be developed further. Fans, dampers and ducting must be integrated into the façade module and in a simple manner connect to the indoor and outdoor environments, and possibly to the adjacent façade modules. Secondly the cooling output from the modules must be increased. This can partially be done by increasing the efficiency of the module, either by improving the optical performance or reducing the thermal losses. The main obstacle to higher outputs however, is the high incidence angles, and as consequence low useful heat input, during summer especially for lower latitudes and south oriented façades. Increasing the heat input would require either changing the slope of the collector, which is difficult in a vertical façade, or introducing external reflectors in front of the collector, possibly as sun shields for the windows below.

The discrepancy between measured and simulated results can actually have a natural explanation. During absorption, condensation in the fluid stream often occurred, but no water was ever seen dripping out of the drain of the collector. The condensate could simply have been evaporated during the consecutive test cycle and so lowered the measured heat output during desorption/condensation. This would then also explain the slow decrease in cooling power towards the end of the absorption phase. Normally the cooling delivery abruptly ends once all refrigerant has been absorbed, but if there is condensate inside the heat exchanger then this water will slowly re-evaporate once the outlet temperature is above the dewpoint of the incoming air, and produce a chilling effect on the air flow. Since the latent power has already been accounted for by comparing the inlet dewpoint with the outlet temperature this additional energy should not be considered in the model. To reduce this discrepancy the model could be updated with a humidity input and a stored variable with the amount of condensed water in the C/E.

Furthermore the model should be included into a complete system model including building, occupants and façade, and used to optimize the concept with respect to orientation, suitable aperture area, control strategy, flow rates etc. Part of this work has been initiated and presented by Avesani et al. in [5].

The further development of the concept must be conducted in close collaboration with a façade manufacturer so that all boundary conditions such as aesthetics, fire protection, structural limits etc. are included in the design. The small size of the prototype collector increased the shadow effects on the 4 sorption tubes as well as decreased the total output capacity of the collector. Further developments should focus on maximizing the aperture area available in the façade module, finding a cost effective solution for the aerualics (fans, dampers, ducting, etc.), and investigating the possibility of increasing the incident irradiation on the collector by horizontal external reflectors.

5. Conclusions

The design goal to have 30Pa pressure drop and similar cooling powers compared to liquid heat transfer are partly achieved. The cooling power and the reactor pressure drop are satisfactory whereas the measured C/E pressure drop is a factor 3 too high. Since the heat exchanger lamella is a standard product and available in many different dimensions it will be fairly simple to adjust the pressure drop in coming prototypes.

The stagnation temperature is significantly lower compared to conventional vacuum tube collectors (220°C at 1000W/m²). Whether this is due to the shorter lengths of the tubes (and hence more edge losses) or because of the quality of the custom made Sydney tubes themselves is beyond the scope of this work.

The simulation model predicts the reality reasonably well. The model constantly over-predicts the condensation heat with on average 5% compared to measurement. At the same time the model under-predicts the cooling output with on average 5%.

The sensitivity study shows similarly to [2] that external and internal losses are main performance drivers. Furthermore it can be seen that the C-C distance is well selected since both adding and subtracting tubes (N_{tube}) lower the efficiency. As expected the cooling output is considerably less for south oriented facades in Rome. This is mainly due to high incidence angles in summer. On higher latitudes, such as Stuttgart, this effect cannot be seen. In general only small improvements on Eta_{cool} can be achieved from a collector optimization perspective. The exception is reducing reactor losses which especially for colder climates still have a large impact.

Acknowledgements

The research leading to these results has received funding from the European Union's Seventh Programme for research, technological development and demonstration under grant agreement No. 314461 –iNSPiRe. The European Union is not liable for any use that may be made of the information contained in this document which is merely representing the authors view. The authors wish to express their gratitude to Swedish Research Council Formas for the financial support to the research leading to the results presented. In addition the authors would like to thank the employees of ClimateWell for building the prototype according to the presented design, P. di Lauro from Fraunhofer ISE for calculating the IAM values and designing the reflector, C. Thoma with the collector testing team for performing the measurements on the collector, and H. Fugmann for the CFD modelling. Finally, we thank Parker for supplying the aluminium lamella heat exchangers free of cost.

References

- [1] Henning Hans-Martin. Solar assisted air conditioning of buildings – an overview. Applied Thermal Engineering, July 2007, vol. 27, 10, p.1734-1749.
- [2] Hallström, O., Földner, G., Spahn H.J., Schnabel L., Salg F., 2014. Development of Collector Integrated Sorption Modules for Solar Heating and Cooling: Performance Simulation. Energy Procedia 48 (2014) 67-76.
- [3] Földner G. et al. KollSorp – Entwicklung eines kollektorintegrierten Sorptionssystems zur solaren Kühlung und Heizungsunterstützung. Proceedings of the 23. Symposium Thermische Solarenergie, OTTI, 2013
- [4] Blackman, C., Hallström, O., Bales, C., 2014, Demonstration of solar heating and cooling system using sorption integrated solar thermal collectors, Conference Proceedings Eurosun 2014, 16-19 September. Aix-les-Bains (France).
- [5] Avesani, S., Hallström, O., Földner, G., 2014, Integration of sorption collector in office curtain wall: Simulation based comparison of different system configurations, Conference Proceedings Eurosun 2014, 16-19 September. Aix-les-Bains (France).